Journal of Engineering Science and Technology
Vol. 13, No. 11 (2018) 3840 - 3855

EFFECT OF VISCOUS HEAT GENERATION ON TEMPERATURE OF RAREFIED GAS MICROFLOWS DRIVEN BY MOVING SURFACE

NAM T. P. LE*, THOAI N. TRAN

Faculty of Mechanical Engineering, Industrial University of Ho Chi Minh City, Vietnam
*Corresponding Author: letuanphuongnam@iuh.edu.vn

Abstract

Good understanding of the gas flow under rarefied conditions is important for designing the micro-electro-mechanical systems. The Navier-Stokes-Fourier equations with the slip and jump conditions can capture the rarefied gas flows in the slip regime. In this paper, we focus on evaluating new type of the Smoluchowski jump condition that was recently proposed in our previous work by considering the viscous heat generation. It was validated for external high-speed rarefied gas flows over the stationary surface. Our investigation is undertaken for internal rarefied gas microflows past the moving surfaces. The lid driven microcavity and Couette cases are adopted for this investigation with Knudsen number ranging from 0.05 to 1, the surface velocity varying from 50 m/s to 200 m/s, and argon as working gas. All simulations are run within the OpenFOAM framework. The gas temperatures along the moving surface and those across the microchannel predicted by new type of the Smoluchowski jump condition are close to the DSMC and R13-moment data in all cases considered

Keywords: Microcavity, New type of Smoluchowski temperature jump condition, Rarefied gas flows, Sliding friction.

1. Introduction

Simulation of rarefied gas flow is important for designing the micro-electro-mechanical systems (MEMS). The rarefied gas flow in MEMS has been considered due to the advent of miniaturization and advances in manufacturing technology [1]. A good understanding of the gas flow under rarefied conditions will aid a lot for an efficient design. MEMS have been worked in different flow regimes that can be described by the Knudsen numbers, Kn. This number is defined as the ratio of molecular mean free path to the macroscopic length scale of the flow. Based on the Kn four flow regimes are distinguished in rarefied gas dynamics: free molecular ($Kn \geq 10$), transition ($0.1 \leq Kn \leq 10$), slip ($0.01 \leq Kn < 0.1$) and continuum regimes ($Kn < 0.01$). Two typical methods have been used to simulate the rarefied gas flows as the Direct Simulation Monte Carlo (DSMC) and Computational Fluid Dynamics (CFD) methods.

The DSMC method is an excellent approach that can successfully simulate the rarefied gas flow in all regimes. However, its computational time is extremely large in comparing with the CFD method, which solves the Navier-Stokes-Fourier (NSF) equations. The NSF equations with the slip and jump conditions can simulate the rarefied gas flows in the slip regime ($0.01 \leq Kn < 0.1$), but cannot capture those in the transition regime ($0.1 \leq Kn \leq 10$). The accuracy of the NSF simulations depends on the slip and jump boundary conditions applied to the surfaces. In rarefied gas microflows the slip and jump conditions were used for the CFD simulations such as Maxwell/Smoluchowski [2, 3], Langmuir [4], Langmuir-Maxwell/Langmuir-Smoluchowski [5] and the second-order [6-9] slip/jump conditions.

Since the gas molecules slide over the surface resulting in the appearance of the viscous heat generation (sliding friction). This will generate more heat transfer that should be involved in derivation of the temperature jump condition. The prediction of the surface gas temperature can depend on a combination of various flow factors such as surface velocity, viscous heat generation, and compressibility which conventional flow models cannot reliably predict [1]. Maslen [10] first introduce the heat transfer generated by the sliding friction and computed based on the inner product of the slip velocity and shear stress at the surface. Le et al. [11] reported the new type of the Smoluchowski jump condition was recently proposed by including the sliding friction term into the standard Smoluchowski jump condition in our previous work. This new jump condition was evaluated for external high-speed rarefied gas flows over the stationary surface.

In the present work, we focus on evaluating new type of the Smoluchowski jump condition for internal rarefied gas flows that are driven by the moving surfaces to investigate the effect of the viscous heat generation on the surface gas temperature past the moving surfaces, and temperature distribution across the microchannel. According to Le at al. [5], moreover, the second order temperature jump condition is also adopted to evaluate for these flows. The lid driven cavity and Couette gas microflow cases are selected for investigation because they are often considered as benchmark problems for validation [1, 12-15]. According to John et al [1], accurate simulation of nonequilibrium temperature can give critical information to designers toward understanding the thermal characteristics and in determining the cooling strategies of micro-devices.

In the present work, the NSF equations with the slip and jump conditions are used for simulating all cases within the OpenFOAM framework. The lid driven

microcavity cases are investigated for a range of Kn from 0.05 to 1 with lid velocity varying from 50 m/s to 200 m/s. The Couette gas microflows are simulated for a range of Kn from 0.05 to 0.5 with the surface velocity $\boldsymbol{u}_w$ = ±100 m/s. Our CFD simulation results of the gas temperatures are compared with the DSMC and *R*13-moment data [1, 12, 13]. We investigate new type of the Smoluchowski jump condition for the lid driven microcavity case at Kn = 0.5 and 1 to verify whether our new Smoluchowski jump condition can predict the gas temperatures of the gas microflows near the moving surface region in the transition regime ($0.1 \leq \text{Kn} \leq 1$).

2. Governing Navier-Stokes-Fourier (NSF) equations

In this section the NSF governing equations are presented. The NSF equations neglecting the body forces are typically used to describe gas flows in the continuum fluid regime, and are expressed in the vector form as follows:

Conservation of mass

$$\frac{\partial \rho}{\partial t} + \nabla \cdot \left[\rho \boldsymbol{u}\right] = 0, \tag{1}$$

Conservation of momentum

$$\frac{\partial (\rho \boldsymbol{u})}{\partial t} + \nabla \cdot \left[\boldsymbol{u}(\rho \boldsymbol{u})\right] + \nabla p + \nabla \boldsymbol{\Pi} = 0, \tag{2}$$

Conservation of total energy

$$\frac{\partial (\rho E)}{\partial t} + \nabla \cdot \left[\boldsymbol{u}(\rho E)\right] + \nabla \cdot (\boldsymbol{u}p) + \nabla \cdot (\boldsymbol{\Pi} \cdot \boldsymbol{u}) + \nabla \cdot \boldsymbol{Q} = 0, \tag{3}$$

where E is total energy, $E = e + 0.5|\boldsymbol{u}^2|$ | with $e = c_v T$; $\boldsymbol{\Pi}$ is stress tensor, $\boldsymbol{\Pi} = -2\mu dev(\boldsymbol{D})$, where$(\boldsymbol{D}) = 0.5[\nabla \boldsymbol{u} + (\nabla \boldsymbol{u})^{\mathrm{T}}]$; *dev* denotes deviatoric of tensor $(\boldsymbol{D})$ - $(1/3)(\mathrm{tr})(\boldsymbol{D})\boldsymbol{I}$; T is the transpose; and $\boldsymbol{Q}$ is computed by the Fourier law, $\boldsymbol{Q} = -k\nabla T$.

A calorically perfect gas is used for all CFD simulations, so $p = \rho RT$ where R is the specific gas constant. According to Greenshields et al. [16], the NSF equations are implemented and solved numerically with the high-resolution central scheme described in OpenFOAM as the solver *rhoCentralFoam*. OpenFOAM is an open source CFD software that uses finite volume numerics to solve systems of partial differential equations ascribed on any 3-dimensional unstructured mesh of polygonal cells.

3. Nonequilibrium boundary conditions in CFD and DSMC

In this section, we revisit nonequilibrium conditions in CFD such as the Maxwell and Smoluchowski boundary conditions, second-order temperature jump condition and new type of the Smoluchowski temperature jump condition. The temperature jump calculation in DSMC is also described.

3.1. Nonequilibrium boundary conditions in CFD

According to Von Smolan [3] and Le et al. [11], in previous work, the standard Smoluchowski temperature condition was modified by considering the viscous heat generation of the rarefied gas flow past a surface. Maslen [10] reported that the

viscous heat generation is calculated by the slip velocity and shear stress terms at the surface. These terms appeared in slip boundary conditions of the moment method [12, 15]. However, the heat transfer normal to the surface in the Smoluchowski theory is calculated by the Fourier law. Maslen [10] stated that when there is slip, heat transfer has two parts: the first part due to conduction and the second part due to viscous heat generation. Latter part is omitted in the Smoluchowski theory, and represents the work done directly on the surface by the shear. It is nonzero only if there is some slip at the surface [10]. Bartz and Vidal [17] and Le et al. [18] explained that the viscous heat generation part in heat transfer was derived from the kinetic theory of gas. Then the heat transfer over the surface considering viscous heat generation was embedded in the Smoluchowski theory to modify the standard Smoluchowski jump condition. According to Le et al. [11], new type of the Smoluchowski jump condition was expressed as follows:

$$T+\frac{\gamma 2\lambda}{Pr(\gamma+1)}\left(\frac{2-\sigma_T}{\sigma_T}\right)\nabla_{\mathbf{n}}T=T_W-\left(\frac{2-\sigma_T}{\sigma_T}\right)\frac{2\lambda}{\mu(\gamma+1)c_v}\left(\boldsymbol{S}\cdot\boldsymbol{n}\cdot\left(\boldsymbol{\Pi}\cdot\left(\boldsymbol{u}-\boldsymbol{u}_w\right)\right)\right) \tag{4}$$

where T_w is the wall temperature. The coefficient σ_T is thermal accommodation coefficient ($0 \leq \sigma_T \leq 1$), perfect energy exchange between the gas and the solid surface corresponds to $\sigma_T = 1$, and no energy exchange to $\sigma_T = 0$; tensor $\boldsymbol{S} = \boldsymbol{I} - \boldsymbol{nn}$, where $\boldsymbol{n}$ is the unit normal vector defined as positive in the direction pointing out of the surface, removes normal components of stresses.

The second term in the right side of Eq. (4) is the viscous heat generation part. This term involves the slip velocity, surface velocity and the shear stress. Based on studies by Le et al. [11], Eq. (4) was investigated for the external rarefied gas flow past the stationary surface ($u_w = 0$) and gave good simulation results. In the current study, Eq. (4) is now evaluated for internal rarefied gas microflow driving by the moving surfaces. The Maxwellian mean free path, λ, and the Sutherland viscosity, μ, are calculated as follows [19]

$$\lambda=\frac{\mu}{\rho}\sqrt{\frac{\pi}{2RT}}, \tag{5}$$

and

$$\mu=A_S\frac{T^{1.5}}{T+T_S}, \tag{6}$$

where $A_S = 1.93\times10^{-6}$ Pa s $K^{-1/2}$ and $T_S = 142$K for argon [5].

In order to compare the simulation results using new type of the Smoluchowski temperature jump condition. The standard Smoluchowski [3] and the second order [5] jump conditions are also adopted for CFD simulations.

The standard Smoluchowski temperature jump [3] condition can be written as

$$T+\frac{2-\sigma_T}{\sigma_T}\frac{2\gamma}{(\gamma+1)Pr}\lambda\nabla_{\mathbf{n}}T=T_w, \tag{7}$$

and the second order temperature jump condition recently proposed in our previous work [5], is also adopted for simulating the lid driven micro cavity and Couette flows. It is expressed as follows [5],

$$T + \frac{2\gamma}{\gamma + 1}\frac{1}{Pr}\left(C_1\lambda\nabla_n T + C_2\lambda^2\nabla_n^2 T\right) = T_w, \tag{8}$$

where C_1 and C_2 are the first and second order coefficients, and are the free parameters. It is seen that since $C_1 = 1$ and $C_2 = 0$ then Eq. (8) becomes the standard Smoluchowski jump condition with $\sigma_T = 1$ in Eq. (7).

Finally, the Maxwell slip velocity condition is selected for all CFD simulations, and is addressed as follows [2]:

$$\mathbf{u} + \left(\frac{2-\sigma_u}{\sigma_u}\right)\lambda\left(\mathbf{S}\cdot\nabla_n\mathbf{u}\right) = \mathbf{u}_w - \left(\frac{2-\sigma_u}{\sigma_u}\right)\frac{\lambda}{\mu}\mathbf{S}\cdot\left(\mathbf{n}\cdot\mathbf{\Pi}_{mc}\right) - \frac{3}{4}\frac{\mu}{\rho}\frac{\mathbf{S}\cdot\nabla T}{T}, \tag{9}$$

where $\boldsymbol{\Pi}_{mc} = \mu((\nabla\boldsymbol{u})^{\mathrm{T}} - \left(\frac{2}{3}\right)\boldsymbol{I}tr(\nabla\boldsymbol{u}))$ is the tensor. The right-hand side of Eq. (9) contains three terms that are associated with (in order): the wall velocity, the so-called curvature effect, and thermal creep. The tangential momentum accommodation coefficient, σ_u, determines the proportion of molecules reflected from the surface specularly (equal to 1-σ_u) or diffusely (equal to σ_u), and $0 \leq \sigma_u \leq 1$.

Equations (4), (7), (8) and (9), can be expressed according to the parameter Kn if we make a nonidmensionalization with the reference length, velocity and temperature for them. Based on Kn, reader can refer to the nondimensional forms of Eqs. (4) and (7). The nonequilibrium boundary conditions presented in Eqs. (4), (7), (8) and (9) are implemented in OpenFOAM to employ with the solver 'rhoCentralFoam'. The implemented approach of nonequilibrium boundary condition was fully described in our previous work [5].

3.2. Temperature jump in DSMC

The surface boundary condition in the DSMC method simulates gas-surface interactions: DSMC particles are adsorbed on the surface and then re-emitted. In fact, DSMC particles collide with the surface, and experience both specular and diffuse interactions. The accommodation coefficient represents the fraction of incoming DSMC particles that is reflected diffusely, and the remainder is reflected specularly. Lofthouse et al. [20] presented the translational temperature jump and is calculated with the accommodation coefficient of unity.

$$T = \frac{\sum\left(\left(m/u_n\right)\left\|\boldsymbol{u}^2\right\|\right) - \sum\left(m/u_n\right)\boldsymbol{u}_s^2}{3k\sum\left(1/u_n\right)} - T_w. \tag{10}$$

where u_n is the velocity normal to the surface; u_s is the slip velocity in DSMC; m is molecular mass; and $||\boldsymbol{u}||$ is the velocity magnitude. The u_n in Eq. (10) is taken prior to and after the collision with the surface, and the summations include pre- and post-collision molecules.

In CFD, the standard Smoluchowski temperature jump condition, Eq. (7), has been computed by the temperature gradient normal to the surface only whereas that of DSMC has been calculated as a function of velocities, Eq. (10). Le et al. [11] commented that the new type of the Smoluchowski jump condition, Eq. (4) is now

complemented the viscous heat generation term and gave good predictions of the surface gas temperatures for external rarefied gas flows past the stationary surfaces.

4. Simulation Results and Discussions

The rarefied gas flows are driven by the moving lid, that moves with a constant lid velocity u_w from left to right while the other three walls are at rest. The gas flows will be investigated in the slip and transition regimes that are indicated by the Knudsen numbers from 0.05 to 1. The gas microflows also experience the separation and reattachment at the top left and right corners, respectively. Separation and reattachment are two important features of the internal flows. These features have an important effect on the heat transfer characteristic [12]. The Couette gas microflows are investigated in the range of Kn from 0.05 to 0.5. The surfaces of the microchannel are moving and the gas moves as the results of shear stress diffusion from the surfaces. In CFD simulations the slip and jump boundary conditions are applied for (T, u) at the surfaces, and zero normal gradient condition is set for pressure, p. For all cases, initial pressure, p_0, and temperature, T_0, are set as initial values in the computational domain, shown in Figs. 1 and 2.

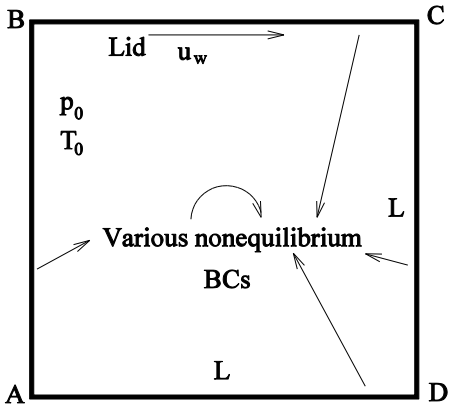

Fig. 1. Numerical setup of the lid driven microcavity case.

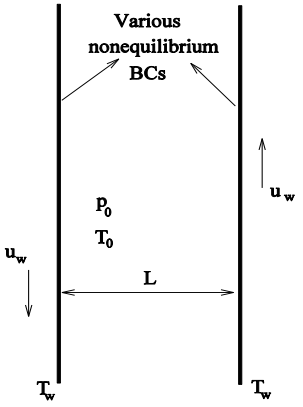

Fig. 2. Numerical setup of the Couette case.

The freestream conditions, final number of cells in computational domain, and Kn numbers of all cases are given in Table 1. Working gas is argon for all cases considered. The accommodation coefficients $\sigma_u = \sigma_T = 1$ are used for our all CFD simulations and the DSMC data [1, 12]. The second order temperature jump condition is employed with the fixed value $C_1 = 1$ and various values of C_2 varying from 0.1 to 0.5.

In the NSF simulations, the slip velocity condition independently works with the temperature jump condition. In a case, if the Maxwell slip condition is employed with various temperature jump conditions then the slip velocities are the same in simulations. This was proved in our previous work [21]. Therefore, we only present the surface gas temperatures over the lid surface for the microcavity cases, and temperature distributions across the microchannel for the Couette gas microflow cases.

Table 1. Freestream conditions, Knudsen number, and cells of all cases.

	p_o (Pa)	u_{wall} (m/s)	T_o (K) = T_w (K)	Kn = λ_0/L	Cell sizes
Cavity 1 [12]	142072	100	273	0.05	200×200
Cavity 2 [1]	10025	50	273	0.5	200×200
Cavity 3 [1]	5012	50; 100; 200	273	1	200×200
Couette [13]	101325	± 100	273	0.05;0.1;0.5	100×400

4.1. Microcavity case 1: u_w = 100 m/s, Kn = 0.05 [12]

Figure 3 shows the surface gas temperatures along the lid surface of the case Kn = 0.05. The NSF simulation with the standard Smoluchowski temperature jump condition is incapability for predicting the surface gas temperatures at the middle of the slip regime, and obtains the lowest values. The surface gas temperatures predicted by new type of the Smoluchowski jump condition and the second order jump condition with C_1 = 1 and C_2 = 0.5 are better than those of the standard Smoluchowski jump condition at the top left (x/L = 0) and right corners (x/L = 1), and are close to the DSMC [12] data along the lid surface. Comparing the simulation results between the standard Smoluchowski and new type of the Smoluchowski jump conditions, the increase of the surface gas temperatures along the lid surface is mostly due to the viscous heat generation. The simulation result of the second order temperature jump condition with C_1 = 1 and C_2 = 0.5 gives good agreement with the DSMC data in the range x/L < 0.6. New type of the Smoluchowski jump condition gives the surface gas temperatures better than those of the second-order conditions for $x/L \geq 0.6$ in comparing with the DSMC data. Their average errors are 0.25% and 0.42%, respectively.

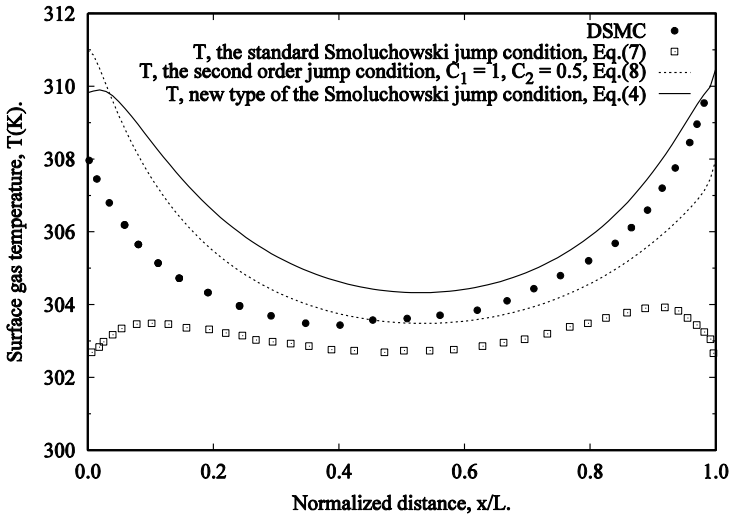

Fig. 3. Surface gas temperature along the lid surface, Kn = 0.05, u_w = 100 m/s.

Our new type of the Smoluchowski temperature jump condition provides more accurate boundary condition and validates on the region near the moving surface. The limited validity of the NSF approach in high Knudsen numbers (Kn ≥ 0.1) still

exists in other region that new jump model does not apply to. So we only show heat flux fields of the microcavity case of Kn = 0.05.

Figure 4 presents the heat flux stream traces overlaid on temperature contour in the cavity for the case Kn = 0.05. This shows at the top left and right corners where the separation and recirculation occur. It is observed that all temperature contours predicted by the NSF equations with various temperature jump conditions are completely different from the DSMC temperature contour [12]. For this case, an expansion cooling (gas temperature T less than the wall temperature T_w, $T < T_w$) does not occur in the cavity for both NSF and DSMC solutions. The peak temperature of the NSF solution with the second order jump condition (T = 365K) is greater than that predicted by the standard Smoluchowski (T = 305K) and the new type of the Smoluchowski jump conditions (T = 311 K). The latter one is close to that of DSMC (T = 309 K). It is also noted the direction of heat transfer is generally from the hot region to the cold region for all NSF solutions. For DSMC solution, the reduction of the gas temperature near the top left wall indicates that the expansion of rarefied gas flow in this region dominates the existing heat transfer mechanism. It is observed that the direction of DSMC heat transfer is found to be from the cold region to the hot region in the upper half of the cavity [12].

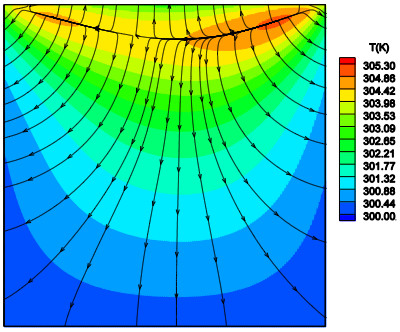

(a) Smoluchowski condition.

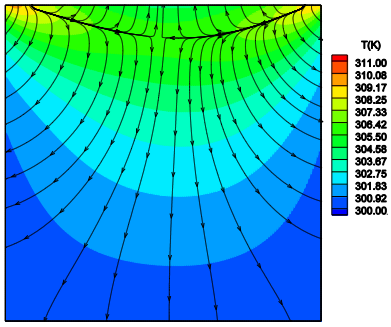

(b) New type of Smoluchowski condition.

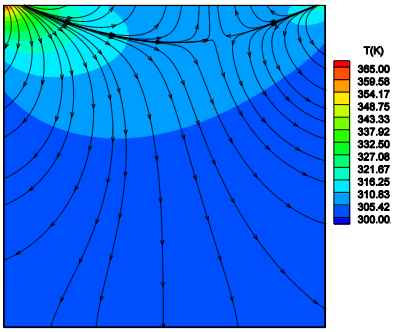

(c) Second-order C_1 = 1, C_2 = 0.5.

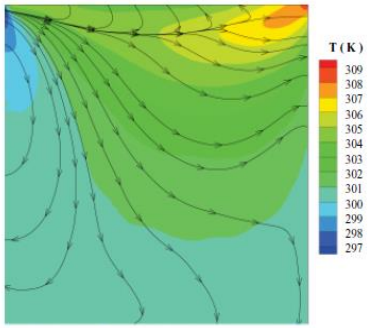

(d) DSMC [12].

Fig. 4. Heat flux in the micro-cavity, Kn = **0.05.**

4.2. Microcavity case 2: u_w = 50 m/s, Kn = 0.5 [1]

Figure 5 presents the surface gas temperatures along the lid surface, for the case Kn = 0.5. The DSMC data [1] gradually increase along the lid surface from the separation region (x/L = 0) to recirculation region (x/L = 1). The temperature predicted by the standard Smoluchowski jump condition is nearly finite constant value along the lid surface, and obtains the lowest values. The temperature predicted by new type of the Smoluchowski jump condition slightly increases along the lid surface, and generally agrees with the DSMC data.

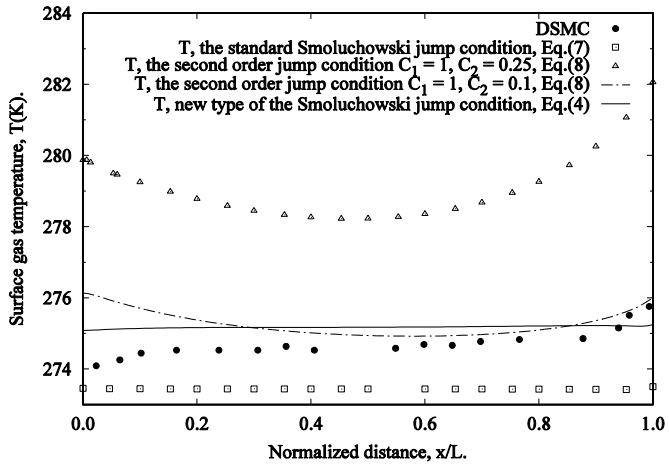

Fig. 5. Surface gas temperature along the lid surface, Kn **= 0.5,** u_w **= 50 m/s.**

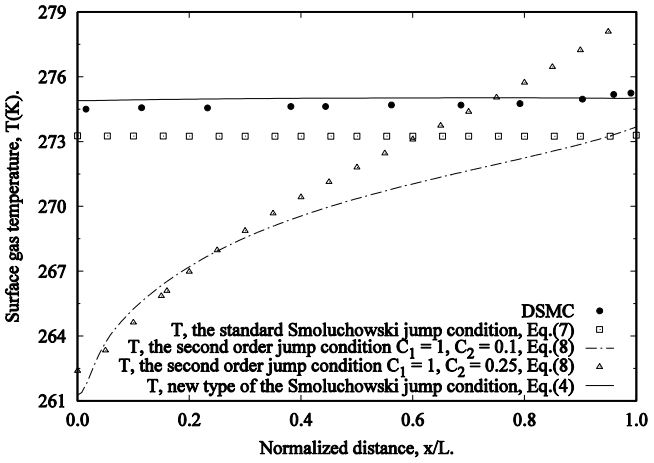

Fig. 6. Surface gas temperature along the lid surface, Kn **= 1,** u_w **= 50 m/s.**

In this case the second order jump condition is investigated with the fixed value C_1 = 1, and two values C_2 = 0.5 and C_2 = 0.1. The second order jump condition with the value C_2 = 0.5 overpredicts the temperatures in comparing with DSMC data, while those using the second order jump condition with C_2 = 0.1 are close to DSMC data. New type of the Smoluchowski jump condition predicts the surface gas temperatures better than those of the second order jump condition with C_2 = 0.1 for $x/L \leq 0.27$ in comparing with the DSMC data.

4.3. Microcavity cases 3: Kn = 1, u_w = 50 m/s, 100 m/s and 200 m/s [1]

Figures 6, 7 and 8 present the surface gas temperatures over the lid surface of the case Kn = 1 with various lid velocities u_w = 50, 100 and 200 m/s. The DSMC data [1] gradually increase along the lid surface in simulations with u_w = 50 m/s and u_w = 100 m/s. They obtain the lowest values at the separation region and highest values at the recirculation region, seen in Figs. 6 and 7.

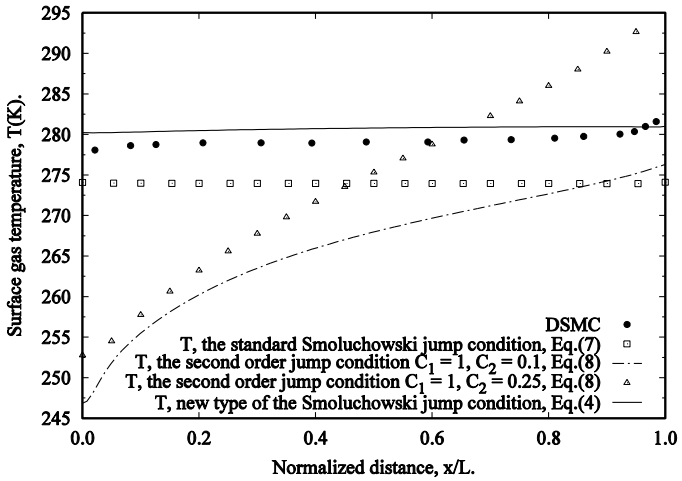

Fig. 7. Surface gas temperature along the lid surface, Kn = 1, u_w = 100 m/s.

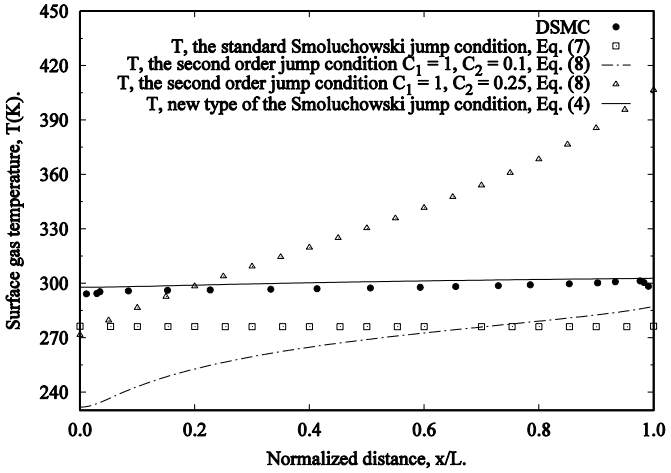

Fig. 8. Surface gas temperature along the lid surface, Kn = 1, u_w = 200 m/s.

The simulation results using new type of the Smoluchowski jump condition slightly raise up along the lid surface while those of the standard Smoluchowski jump condition are nearly finite constant values. In both of cases, the temperatures predicted by new type of the Smoluchowski jump condition are close to DSMC data, while those of the standard Smoluchowski jump condition are not.

For the case u_w = 200 m/s the DSMC data [1] gradually increase along the lid surface until x/L = 0.98 before decreasing in $0.98 \leq x/L \leq 1$. The temperatures using new type of the Smoluchowski jump condition gradually raise up along the lid surface while those of the standard Smoluchowski jump condition are nearly a finite constant value, as seen in Fig. 8. The surface gas temperature using new type of the Smoluchowski jump condition is close to the DSMC data while those using the standard Smoluchowski jump condition is not. For all cases Kn = 1, the second order temperature jump condition cannot predict the surface gas temperatures in comparing with the DSMC data.

4.4. Couette cases: u_w = ±100 m/s, Kn = 0.05, 0.1 and 0.5 [13]

Figures 9, 10 and 11 present the normalized gas temperature (T/T_w) distribution across the microchannel of the Couette cases with various Kn = 0.05, 0.1 and 0.5. The CFD results with the standard Smoluchowski, new type of the Smoluchowski, and the second order jump conditions are compared with the DSMC and R13-moment data [13]. Their distributions are symmetrical through the center-line of the microchannel. Since Kn increases the temperature raises up significantly, and the curvature of the temperature distribution profile reduces.

The increase of temperature can be explained that molecules near the surfaces and the center-line of the microchannel can collide with the surfaces when the length of the micro-channel width, L, decreases. In Fig. 9, the case Kn = 0.05, new type of the Smoluchowski jump condition predicts the surface gas temperature close to the DSMC data [13] while the standard Smoluchowski condition data does not. The simulation results using new type of the Smoluchowski jump condition and the second order jump condition with C_1 = 1 and C_2 = 0.5 are close to the DSMC data.

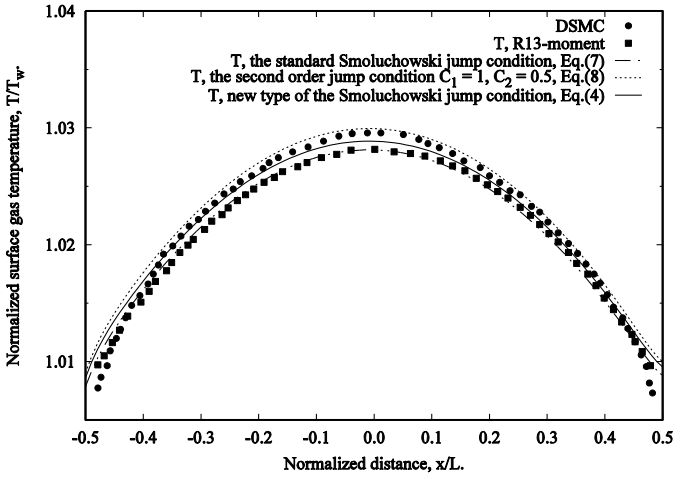

Fig. 9. Normalized gas temperature distribution across the microchannel, Kn = 0.05.

In Fig. 10, Kn = 0.1 the simulation results using new type of the Smoluchowski and the second-order jump (C_1 = 1 and C_2 = 0.5) conditions are better than those of the standard Smoluchowski jump condition and *R*13-moment results in comparing with the DSMC data. The temperature predicted by the standard Smoluchowski condition obtains lowest values near the center-line. In Fig. 11, Kn = 0.5, the

simulation results of the standard Smoluchowski condition obtains the lowest values. The temperatures predicted by new type of the Smoluchowski jump condition and the *R*13-moment method are close together and give reasonable agreement with DSMC data. The second order jump condition with the values C_1 = 1 and C_2 = 0.5 overpredicts the gas temperatures in comparing with DSMC data. A reduction of the value C_2 = 0.1 leads to the good agreement between the simulation results of the second order jump condition and the DSMC data.

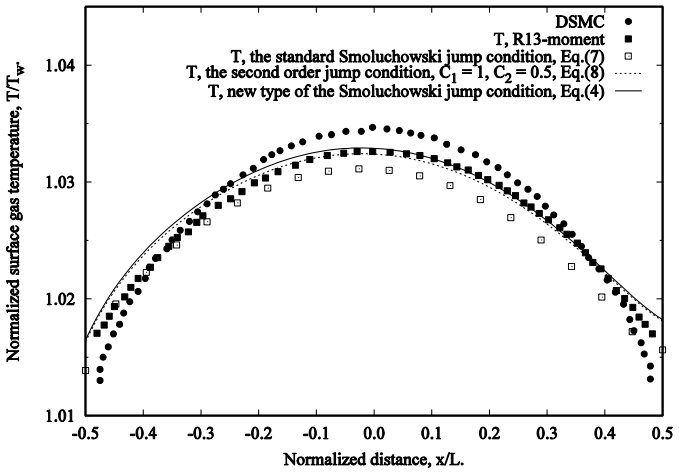

Fig. 10. Normalized gas temperature distribution across the microchannel, Kn = 0.1.

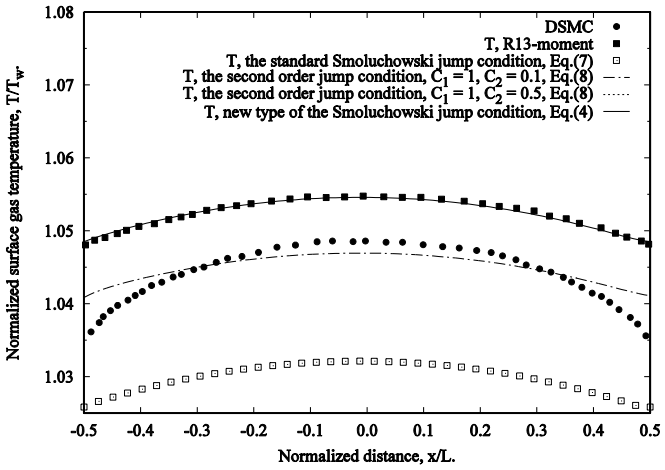

Fig. 11. Normalized gas temperature distribution across the microchannel, Kn = 0.5.

4.5. Discussions

From the simulation results obtained, the increase of the lid velocity, $\boldsymbol{u}_w$, leads to the increase of the surface gas temperature significantly, especially for the case with $\boldsymbol{u}_w$ = 200 m/s. The appearance of the viscous heat generation term calculated by the inner

product of the slip velocity and shear stress in new type of the Smoluchowski jump condition results in the agreement between the CFD surface gas temperatures and the DSMC data [1] of the microcavity cases Kn = 0.5 and 1. The surface gas temperatures predicted by the standard Smoluchowski jump condition generally do not agree with the DSMC data because they are calculated by the temperature gradient only. Since the lid is moving we have $T > T_w$ which is due to the viscous heat generation. Considering all microcavity cases, the viscous heat generation plays an important role for predicting the surface gas temperatures along the lid surface, and reduces the gap of those between the DSMC and the NSF simulations.

For two cases u_w = 50 m/s with Kn = 0.5 and 1, the addition of viscous heat generation in the temperature jump condition affects the gas temperature near region of the moving lid, and predicts the peak temperature close to that of DSMC. Le et al. [11] proved that new type of the Smoluchowski jump condition can capture the surface gas temperature for external rarefied gas flow over NACA0012 micro-airfoil at Kn = 0.26. The surface gas temperatures using new jump condition along the lid of the microcavity cases at Kn = 0.5 and 1 are close to the DSMC data [1, 12].

For the Couette gas microflow cases, the simulation results show that the effect of viscous heat generation is significant to predict the temperature distribution across the microchannel, and improves the simulation results in comparing with DSMC data. Since Kn increases, the standard Smoluchowski condition cannot predict the temperature distribution while new type of the Smoluchowski jump condition can. The surface gas temperatures of the *R*13-moment method and new type of the Smoluchowski jump condition (case Kn = 0.5) are close together. This may be explained that the temperature jump condition in *R*13-moment method also includes the terms of shear stress and velocity [15]. They significantly affect the temperature distribution across the microchannel for the case Kn = 0.5.

By adding the normal temperature gradient in the second order term, the second order temperature jump can capture the surface gas temperatures along the lid of the cavity and temperature distribution across the microchannel for the Couette microflows up to Kn of 0.5 However, the use of the second order jump condition depends on the selected value of the coefficient C_2 to match the given DSMC data. The second order jump condition cannot predicted the surface gas temperatures for the microcavity case Kn = 1 due to the effect of high rarefaction. Moreover, the surface gas temperature predicted by the second order jump condition is computed by the temperature gradient only while the prediction of that may depend on a combination of various flow factors such as surface velocity, viscous heat generation, and compressibility. The viscous heat generation may significantly affect the surface gas temperature under nonequilibrium flow conditions. This results in the surface gas temperatures predicted by new type of the Smoluchowski jump condition are close to the DSMC data for the microcavity case Kn = 1.

5. Conclusion

Le et al. [11] proposed the new type of the Smoluchowski jump condition, which has been evaluated for internal rarefied gas flows in the lid driven cavity and Couette gas microflows. The term of viscous heat generation included in new type of the Smoluchowski jump condition shows that the NSF equations can predict the

surface gas temperatures along the lid surface in the transition regime ($0.1 \leq Kn \leq 1$), and temperature distribution across the microchannel ($Kn \leq 0.5$) close to the DSMC data whereas those with the standard Smoluchowski jump condition cannot. The second order jump condition can simulate the gas temperatures up to Kn of 0.5 for both the cavity and the Couette gas microflow cases. Le et al [11] figure out that the new type of the Smoluchowski jump condition physical insight as the effect of the viscous heat generation on the surface gas temperature, which past the moving surface as well as temperature distribution across the microchannel and provides more accurate boundary conditions. It should be used for predicting the surface gas temperature along the moving surface in both the slip and transition regimes in CFD for the lid-driven cavity and Couette gas microflows.

Nomenclatures

A_S	Constant for Sutherland's law, Pa s/K$^{-0.5}$
c_p	Specific heat of a gas at constant pressure, J/kg·K
c_v	Specific heat of a gas at constant volume, J/kg·K
e	Internal energy, J/kg
E	Energy, J
I	Identify tensor
k	Thermal conductivity, W/m·K
Kn	Knudsen numbers
n	Surface normal vector
Pr	Prandtl number
p	Gas pressure, Pa
Q	Surface heat flux
R	Specific constant of gas, m^2/s^2·K
S	Transformation tensor
T	Temperature, K
T_S	Constant temperature, K
T_w	Wall temperature, K
tr	Trace
$\boldsymbol{u}$	Velocity, m/s
$\boldsymbol{u}_w$	Wall velocity, m/s

Greek Symbols

γ	Specific heat ratio
λ	Mean free path, m
μ	Dynamic viscosity, Pa s
$\boldsymbol{\Pi}$	Stress tensor
$\boldsymbol{\Pi}_{mc}$	Curvature effect
ρ	Density, kg/m^3
σ_T	Thermal accommodation coefficient, ($0 \leq \sigma_T \leq 1$)
σ_u	Tangential momentum accommodation coefficient, ($0 \leq \sigma_u \leq 1$)

Abbreviations

CFD	Computational Fluid Dynamics
DSMC	Direct Simulation Monte Carlo
NSF	Navier Stokes Fourier

References

1. John, B.; Gu, X.-J.; and Emerson, D.R. (2010). Investigation of heat and mass transfer in a lid-driven cavity under nonequilibrium flow conditions. *Numerical Heat Transfer, Part B: Fundamentals*, 58(5), 287-303.
2. Maxwell, J.C. (1879). On stresses in rarefied gases arising from inequalities of temperature. *Philosophical Transactions of the Royal Society*, 170, 231-256.
3. Von Smolan, R.M.S. (1898). Uber Warmeleitung in verdunnten gasen. *Annalen der Physik*, 300(1), 101-130.
4. Myong, R.S. (2004). Gaseous slip models based on the Langmuir adsorption isotherm. *Physics of Fluids*, 16(1), 104-117.
5. Le, N.T.P.; White, C.; Reese, J.M.; and Myong, R.S. (2012). Langmuir-Maxwell and Langmuir-Smoluchowski boundary conditions for thermal gas flow simulations in hypersonic aerodynamics. *International Journal of Heat and Mass Transfer*, 55(19-20), 5032-5043.
6. Deissler, R.G. (1964). An analysis of second order slip flow and temperature jump boundary conditions for rarefied gases. *International of Journal Heat and Mass Transfer*, 7(6), 681-694.
7. Le, N.T.P.; and Roohi, E. (2015). A new form of the second order temperature jump boundary condition in the low speed nano/microscale and hypersonic rarefied gas flow simulations. *International Journal of Thermal Sciences*, 98, 51-59.
8. van Rij, J.; Ameel, T.; and Harman, T. (2009). The effect of viscous dissipation and rarefaction on rectangualar microchannel convective heat transfer. *International Journal of Thermal Sciences*, 48(2), 271-281.
9. Karniadakis, G.E.; Beskok, A.; and Aluru, N. (2005). *Microflows and nanoflows.* Fundamentals and Simulation. New York: Springer-Verlag.
10. Maslen, S.H. (1958). On heat transfer in slip flow. *Journal of the Aerospace Sciences*, 25(6), 400-401.
11. Le, N.T.P.; Vu, N.A.; and Loc, L.T. (2017). New type of Smoluchowski temperature jump condition conidering the heat viscous generation. *AIAA Journal*, 55(2), 474-483.
12. Mohammadzadeh, A.; Roohi, E.; Niazmand, H.; Stefanov, S.; and Myong, R.S. (2012). Thermal and second-law analysis of a micro- or nanocavity using direct-simulation Monte Carlo. *Physical Review E*, 85(5), 11 pages.
13. Taheri, P.; Torrilhon, M.; and Struchtrup, H. (2009). Couette and Poiseuille microflows: Analytical solutions for regularized 13-moment equations. *Physics of Fluids*, 21(1), 11 pages.
14. Marques, W.; Kremer, G.M.; and Sharipov, F.M. (2000). Couette flow with slip and jump boundary conditions. *Continuum Mechanics and Thermodynamics*, 12(6), 379-386.
15. Rana, A.S.; Mohammadzadeh, A.; and Struchtrup, H. (2015). A numerical study of the heat transfer through a rarefied gas confined in a microcavity. *Continuum Mechanics and Thermodynamics*, 27(3), 433-446.
16. Greenshields, C.J.; Weller, H.G; Gasparini, L.; and Reese, J.M. (2010). Implementation of semi-discrete, non-staggered central schemes in a

colocated, polyhedral, finite volume framework, for high-speed viscous flows. *International Journal for Numerical Methods in Fluids*, 63(1), 1-21.

17. Bartz J.A.; and Vidal R.J. (1969). Surface measurements on sharp flat plates and wedges in low-density hypersonic flow. *AIAA Journal*, 7(6), 1099-1109.
18. Le, N.T.P.; Vu, N.A.; and Loc, L.T. (2016). Effect of the sliding friction on heat transfer in high-speed rarefied gas flow simulations in CFD. *International Journal of Thermal Sciences*, 109, 334-341.
19. Kennard, E.H. (1938). *Kinetic theory of gases.* New York: McGraw-Hill Book Company Inc.
20. Lofthouse, A.J.; Scalabrin, L.C.; and Boyd, I.D. (2008). Velocity slip and temperature jump in hypersoni aerothermodynamics. *Journal of Thermophysics and Heat Transfer*, 22(1), 38-49.
21. Le, N.T.P.; Greenshields, C.J.; and Reese, J.M. (2012). Evaluation of nonequilibrium boundary condition in simulating hypersonic gas flows. *Progress in Flight Physics*, 3, 217-230.